

Aquila X–1: a low inclination soft X-ray transient

T. Shahbaz,¹ J.R. Thorstensen,² P.A. Charles,¹ and N.D. Sherman²

¹*Department of Astrophysics, Nuclear Physics Building, Keble Road, Oxford, OX1 3RH, UK*

²*Department of Physics and Astronomy, Dartmouth College, 6127 Wilder Laboratory, Hanover, NH 03755-3528*

9 April 2018

ABSTRACT

We have obtained *I*-band photometry of the neutron star X-ray transient Aql X–1 during quiescence. We find a periodicity at 2.487 c d^{-1} , which we interpret as twice the orbital frequency ($19.30 \pm 0.05 \text{ h}$). Folding the data on the orbital period, we model the light curve variations as the ellipsoidal modulation of the secondary star. We determine the binary inclination to be 20° – 31° (90 per cent confidence) and also 95 per cent upper limits to the radial velocity semi-amplitude and rotational broadening of the secondary star to be 117 km s^{-1} and 50 km s^{-1} respectively.

Key words: binaries: close – stars: individual: Aquila X–1 – stars: neutron – X-rays: stars.

1 INTRODUCTION

Aquila X–1 (=V1333 Aquilae) is a soft X-ray transient source that shows type I X-ray bursts (Koyama et al. 1981; Czerny, Czerny & Grindlay 1987), thereby indicating that the compact object is a neutron star. From quiescent observations the companion star has been identified to be a $V=19.2$ K1IV star (see Shahbaz, Casares & Charles and references within). Aql X–1 is known to undergo regular X-ray and optical outbursts on a timescale of ~ 1 year (Kaluziński et al. 1977; Priedhorsky & Terrell 1984; Charles et al. 1980) much more frequently than the other neutron star transient Cen X–4 (McClintock & Remillard 1990).

Attempts to find the orbital period have revealed many modulations. Watson (1976) reported an unconfirmed 1.3 day X-ray periodicity during the 1975 outburst. Chevalier & Ilovaisky (1991) have obtained an 18.97 hr periodicity from optical photometry during its active state, which they interpret as being the orbital period.

Recently the RXTE All Sky Monitor showed Aql X–1 to have undergone an X-ray outburst between late January and early March 1997 (Levine & Thomas 1997). Ilovaisky & Chevalier (1997) reported that Aql X–1 was optically in quiescence by 30 March 1997. In this letter we report on our *I*-band photometry of Aql X–1 obtained in June 1997, when the source was in quiescence. We are able to confirm the periodicity detected by Chevalier & Ilovaisky (1991) and determine the binary inclination.

2 OBSERVATIONS AND DATA REDUCTION

We monitored Aql X–1 on the nights of 1997 June 20, 23, 24, 25, and 26 UT, using the 1.3 m McGraw-Hill telescope

at Michigan-Dartmouth-MIT (MDM) Observatory and a direct CCD camera equipped with a 1024^2 thinned Tektronix chip which yielded $0''.51 \text{ pixel}^{-1}$ at $f/7.5$. The nights of June 21 and 22 were clear, but the source was too close to the bright moon to observe. To suppress scattered moonlight and to obtain maximum sensitivity to the cool secondary star, an interference filter approximating the Kron-Cousins *I*-band was used for all the exposures, which were generally 480 s long. Except for a very few thin clouds on June 20, conditions were entirely photometric. The seeing was variable but generally usable ($\text{FWHM} < 2''$). Occasional focus changes and tracking problems spoiled a few frames. In order to obtain maximum leverage in the time series analysis we observed Aql X–1 for as long as we could each night.

For flatfield division we used median-filtered exposures of the twilight sky taken the same nights as the data. The flatfield pictures agreed very well from night to night, except for occasional ~ 1 per cent changes in the shadows cast by dust particles on the CCD window. Bias subtraction was accomplished using overscan regions of the picture. For all reductions we used IRAF* routines. We measured eight stars (Table 1) in each picture using the `apphot` package; of a variety of software apertures, a $1.''4$ radius gave the lowest scatter among the *differential* magnitudes, the averages of which are listed in Table 1. Photometric standardization was not attempted. The coordinates in Table 1 are derived from a fit of eight stars from the HST Guide Star Catalog v1.2 in a single good-seeing frame, and are estimated accurate to $< 0''.3$ from the scatter of the fit. The mean differential *I*

* IRAF, the Image Reduction and Analysis Facility, is produced by the National Optical Astronomy Observatories.

Table 1. Differential magnitude and position of local field stars.

RA (J2000)	Dec (J2000)	ΔI (mags)	Comments
19 11 16.06	+0 35 05.6	2.272±0.022	Aql X-1
19 11 16.11	+0 35 13.9	(±0.108)	local standard
19 11 15.61	+0 35 01.0	2.002±0.018	comparison star
19 11 13.99	+0 34 39.9	-0.524±0.009	
19 11 17.03	+0 35 30.5	0.752±0.009	
19 11 17.00	+0 35 22.0	2.576±0.025	
19 11 18.63	+0 35 24.0	3.024±0.038	
19 11 16.83	+0 34 55.9	2.697±0.040	

magnitudes were computed by averaging over all frames and rejecting points more than three standard deviations from the median. For the local standard ($\sim 8''$ north of Aql X-1), only the standard deviation of the instrumental magnitudes is given.

3 THE SEARCH FOR THE ORBITAL PERIOD

We expect the quiescent optical modulation in Aql X-1 to arise primarily from the ellipsoidal variations of the secondary star, as it does in other SXTs. These variations arise since the observer sees differing aspects of the gravitationally distorted star as it orbits the compact object (van Paradijs & McClintock 1995). In theory the modulation should have two maxima and minima. The two minima may be unequal depending on the binary inclination, but the maxima should be equal. However, in practice, the light from the accretion disc (especially in the optical) contaminates the ellipsoidal variations of the secondary star, making detailed interpretations of the optical light curves difficult (see Shahbaz, Naylor & Charles 1993).

Therefore, we first analysed the optical light curve of Aql X-1 using the phase dispersion minimization algorithm (Stellingwerf 1975). This technique is insensitive to the shape of the modulation, but does not remove the effects of the window function. The method groups the data in phase bins and seeks to minimize the dispersion within the bins. The deepest minimum of the statistic is the best estimate of the period. The PDM spectrum was computed in the frequency range 0.1 to 4.0 c d^{-1} at a resolution of 0.01 c d^{-1} with 20 phase bins.

The common method of computing a discrete Fourier transform (DFT) and halving the estimate of the period is equivalent to assuming that the maxima and/or minima are of equal depths. This may not be the case, as the observed ellipsoidal modulation may contain unequal maxima and/or minima depending on the binary inclination and the contamination by the accretion disc. A Lomb-Scargle periodogram (Lomb 1976; Scargle 1982) of the data set was then computed with the same resolution and frequency range as was used for the PDM periodogram.

Figure 1 shows the PDM and Lomb-Scargle periodograms, with three frequencies present at 0.524 c d^{-1} , 1.509 c d^{-1} and 2.487 c d^{-1} . The suggested orbital period of Chevalier & Ilovaisky (1991) is marked at 18.97±0.02 hr. If this is the orbital period, then it should appear in the Lomb-Scargle periodogram as a peak at twice the frequency, *i.e.*

at 2.530 c d^{-1} . In both the PDM and Lomb-Scargle periodograms a periodicity at 2.487 c d^{-1} is present. Chevalier & Ilovaisky's period should also appear in the PDM periodogram, since the method is insensitive to the shape of the modulation in the light curve; a periodicity at 1.242 c d^{-1} is present. We note that no periodicity at 1.242 c d^{-1} or 2.487 c d^{-1} is present in the light curves of the comparison stars. We therefore assume the peak in the Lomb-Scargle periodogram at 2.487 c d^{-1} with a power of 31 to be real.

In Figure 1 we also show the 99 per cent confidence level which allows us to demonstrate the significance on the peaks detected in the Lomb-Scargle periodogram. The level was calculated from a Monte Carlo simulation, which calculates the maximum power in 10 000 sets of Gaussian noise with mean and variance equal to that of Aql X-1. Random peaks reaching a power of 7.8 are only found in 1 per cent of the artificial data sets, hence this defines our 99 per cent confidence level. Thus we conclude that the power level of the 2.487 c d^{-1} peak is substantially greater than 99 per cent level significant. In order to estimate the uncertainty in the 2.487 c d^{-1} peak position we created an artificial data set, with a mean, variance, semi-amplitude, amplitude difference between the minima and baseline equal to that in Aql X-1. The observed ellipsoidal modulation is well represented by a sinusoid of frequency $2f$ which lags 90 degrees in phase, relative to sinusoid at frequency f . The amplitude of the sinusoid at frequency f determines the difference between the minima in the final light curve. Since this difference is small (0.01 mags), the ellipsoidal light curve is very similar to a single sinusoid of frequency $2f$. Using a Monte Carlo simulation we recorded the peak power in the Lomb-Scargle periodogram near the peak of interest, for the artificial data set. This was repeated 10 000 times to produce good statistics, giving a mean peak at 2.487 ± 0.005 c d^{-1} (1- σ uncertainty). Since this peak corresponds to twice the orbital frequency, the orbital period is then 1.244±0.003 c d^{-1} (=19.30±0.05 h).

Chevalier & Ilovaisky (1991) were taken over a 3 month baseline, when Aql X-1 was in its active state. The *V*-band modulation they observe is probably due to a combination of X-ray heating of the secondary star, and of the accretion disc. Modulations of this kind are probably not coherent, due to the highly variable nature of the accretion disc, even more so in the *V*-band (van Paradijs & McClintock 1995). Our observations of Aql X-1 were taken when the source was in quiescence, and where in the *I*-band the accretion disc contribution is negligible (Shahbaz, Casares & Charles 1997). Therefore, what we see in the *I*-band is the characteristic double humped modulation per orbital cycle, due to the ellipsoidal shape of the secondary star. We therefore take the orbital period to be 19.30±0.05 h (=0.804±0.002 d).

From Table 1 it can be seen that the scatter in the Aql X-1 data is similar to stars of comparable brightness. This may suggest that the modulation we have detected is not real. However, it should be noted that we can still use the largest amplitude of an ellipsoidal modulation that could conceivably be hidden within the noise in the data, to constrain the inclination of the system.

4 MODEL FITTING AND DERIVED PARAMETERS

Using an orbital period $P=19.30$ h ($=0.804$ d) we folded the Aql X-1 and comparison star data. As there is no spectroscopic ephemeris defining phase 0.0 (i.e. superior conjunction of the secondary star) we used an arbitrary value for T_0 . We then shifted the light in phase so that the deeper minima corresponded to phase 0.0. [Note that the choice is arbitrary. In the fitting procedure (see later), one of the free parameters is a phase shift.] The data were then binned into 15 phase bins, and the standard error and mean were then calculated for each bin after discarding the data points which were more than $3\text{-}\sigma$ away from the mean of each bin. This process removed 4 and 12 discrepant data points from the Aql X-1 and comparison star data respectively; the total number of data points was 152. Figure 2 shows the resulting light curves for Aql X-1 and a comparison star.

We fitted the orbital I -band light curve of Aql X-1 with an ellipsoidal model, similar to that used for the other objects in our programme (see Shahbaz, Naylor & Charles 1997 and references within). The model describes the light curve generated by a Roche lobe filling star, where each element of area on the surface of the star is assumed to emit blackbody radiation. The temperature distribution over its surface is assumed to vary according to Von Zeipel’s (1924) gravity darkening law and a linear limb darkening law is used. For a detailed description of the model see Shahbaz, Naylor & Charles (1993). The model parameters were the binary mass ratio ($q = M_1/M_2$ where M_1 and M_2 are the mass of the compact object and secondary star respectively), the inclination (i) and the effective temperature of the secondary star (T_{eff}). A bright spot, i.e. the region where the accretion stream hits the accretion disc was also included. The free parameters of the model were a phase shift, the normalisation of the bright spot and the normalisation of the light curve. Thus the fitting procedure is not dependent on the choice for T_0 . We performed least-squares fits to the data using this model, grid searching q in the range 1–10 and i in the range 5° – 50° . A T_{eff} of 4620 K, appropriate for a K1IV star was used. We used a gravity darkening exponent of 0.05; Sarna (1989) finds the gravity darkening exponent for convective stars with $M_2 < 0.7$ to be 0.05. The limb darkening coefficient for the I -band (9000Å) and the varying temperature around the surface of the secondary star was interpolated from the tables given by Al-Naimiy (1978). The best fit gives a χ^2_ν of 1.45 at $q = 3$, $i = 25^\circ$, with a phase shift of $0.0033\phi (=0.027$ d). This fit is plotted in Figure 2 as the dashed line. The phase shift allows us to estimate T_0 to be HJD 2450623.450 \pm 0.016.

Figure 3 shows the resulting (i, q) diagram with the 68 and 90 per cent confidence regions marked, calculated according to Lampton, Margon & Bowyer (1976) for three parameters (the phase shift, bright spot normalisation and the light curve normalisation), after the error bars had been rescaled to give a fit with a χ^2_ν of 1. As one can see, the ellipsoidal variation is only weakly dependent on q . The 68 and 90 per cent confidence regions for the binary inclination are 21° – 30° and 20° – 31° respectively.

Shahbaz, Casares & Charles (1997) determine the fraction of light arising from the accretion disc to be 6 ± 3 per cent at 6000Å. With increasing wavelength the disc contam-

ination decreases (see McClintock & Remillard 1986; Shahbaz, et al. 1996 and references within), therefore the I -band disc contamination should be lower. If we assume a 95 per cent upper limit of 9 per cent for the disc contamination, the effect of this on the binary inclination is to increase it by at most 1° .

From Figure 2 it can be seen that there seems to be some systematic trend in the data of the comparison star. As noted earlier the scatter in the comparison star data is comparable to that in the Aql X-1 data (see also Table 1). If we assume that the modulation we observe in the Aql X-1 data is not due to the ellipsoidal modulation of the secondary star, and what we have fitted is the maximum possible modulation that could be present, then our fits allow us to determine a 95 percent upper limit of 31° to the binary inclination.

5 DISCUSSION

5.1 The period difference

The quiescent period (19.30 h) we find is slightly different (~ 2 per cent) from the outburst period (18.97 h) obtained by Chevalier & Ilovaisky. Outburst and quiescent period differences are observed in SXTs (see O’Donoghue & Charles 1996), but the outburst modulation (caused by the precession of the accretion disc; Whitehurst 1988) is usually a few per cent *longer* than the orbital period. If we interpret Chevalier & Ilovaisky’s outburst period as being due to the superhump phenomenon, then the superhump period is shorter than the orbital period by 2 per cent, i.e. we have a “negative” superhump. This may seem unusual, but negative superhumps have previously been observed in cataclysmic variables, e.g. in V503 Cyg the superhump period is shorter than the orbital period by 3 per cent (Harvey, Skillman, Patterson & Ringwald 1995).

5.2 Upper limits on K_2 and $v \sin i$

We can compare Aql X-1 to the other long period neutron star SXT Cen X-4. Assuming that our inclination is correct, and that both systems have similar mass neutron stars, then one can estimate K_2 , the semi-amplitude of the radial velocity curve for Aql X-1 (K_2 scales with $\sin i$). Using $K_2=146$ km s^{-1} (McClintock & Remillard 1990) and $i = 40^\circ$ for Cen X-4 and $i < 31^\circ$ for Aql X-1, we find $K_2 < 117$ km s^{-1} (95 per cent upper limit) for Aql X-1.

We can also determine the upper limit to the rotational broadening of the secondary star ($v \sin i$) assuming that the secondary star fills its Roche lobe and its spin is tidally locked to the binary period. Eliminating K_2 from the mass function and the equation which relates the rotational broadening to the radial velocity semi-amplitude and mass ratio (Wade & Horne 1986), we obtain the expression

$$v \sin i = 283 \sin i (M_2/P)^{1/3} \text{ km s}^{-1}. \quad (1)$$

The secondary star must be less massive than a main sequence star of the same spectral type, $0.8 M_\odot$. Then using equation (1) with $P=19.3$ hr and $i < 31^\circ$ gives $v \sin i < 50$ km s^{-1} (95 per cent upper limit). This value for $v \sin i$ is

consistent with the limits obtained by Shahbaz, Casares & Charles (1997).

6 CONCLUSION

Using *I*-band photometry of Aql X-1 taken during quiescence, we have detected a periodicity at 2.487 c d^{-1} , which we interpret as twice the orbital frequency. Folding the data on the orbital period ($19.30 \pm 0.05 \text{ hr}$), we fit the ellipsoidal modulation of the secondary star. We determine 95 per cent upper limits to the binary inclination, radial velocity semi-amplitude and rotational broadening of the secondary star to be 31° , 117 km s^{-1} and 50 km s^{-1} respectively.

ACKNOWLEDGEMENTS

The data analysis was carried out on the Oxford Starlink node using the ARK and Starlink software.

REFERENCES

- Al-Naimiy H.M., 1978, *Ap&SS*, 53, 181
 Charles P.A., 1980, *ApJ*, 249, 567
 Chevalier C., Ilovaisky S.A., 1991, *A&A*, 251, L11
 Czerny, M., Czerny, B., Grindlay, J.E., 1987, *ApJ*, 312, 122
 Harvey, D., Skillman D.R., Patterson J., Ringwald F.A., 1995, *PASP*, 107, 551
 Ilovaisky, S.A., Chevalier, C., 1997 *IAU Circ.* 6638
 Kaluzienski, L.J., et al., 1977, *Nat*, 265, 606
 Lampton M., Margon B., Bowyer S., 1976, *ApJ*, 208, 177
 Levine, A.M., Thomas, B., 1997, *IAU Circ.* 6558
 Lomb N.R., 1976, *ApS&S*, 39, 447
 Koyama, K., 1981, *ApJ*, 247, L27
 McClintock J.E., Remillard R.A., 1986, *ApJ*, 308, 110
 McClintock, J.E., Remillard, R.A., 1990, *ApJ*, 350, 386
 O'Donoghue D., Charles P.A., 1996, *MNRAS*, 282, 191
 Priedhorsky, W.C., Terrell, J., 1980, *ApJ*, 280, 661
 Sarna M.J., 1989, *A&A*, 224, 98
 Scargle J.D., 1982, *ApJ*, 263, 835
 Shahbaz T., Naylor T., Charles P.A., 1993, *MNRAS*, 265, 655
 Shahbaz T., Bandyopadhyay R., Charles P.A., Naylor T., 1996, *MNRAS*, 282, 977
 Shahbaz T., Naylor T., Charles P.A., 1997, *MNRAS*, 285, 607
 Shahbaz T., Casares J., Charles P.A., 1997, *A&A*, 326, L5
 Stellingwerf R.F., 1975, *ApJ*, 224, 953
 van Paradijs J., McClintock J.E., 1995, in *X-ray Binaries*, eds, Lewin W H.G., van Paradijs J., and van den Heuvel E.P.J., CUP, p 58
 von Zeipel H., 1924, *MNRAS*, 84, 665
 Wade R.A., Horne K., 1988, *ApJ*, 324, 411
 Watson, M.G., 1976, *MNRAS*, 176, 19
 Whitehurst R., 1988, *MNRAS*, 233, 529

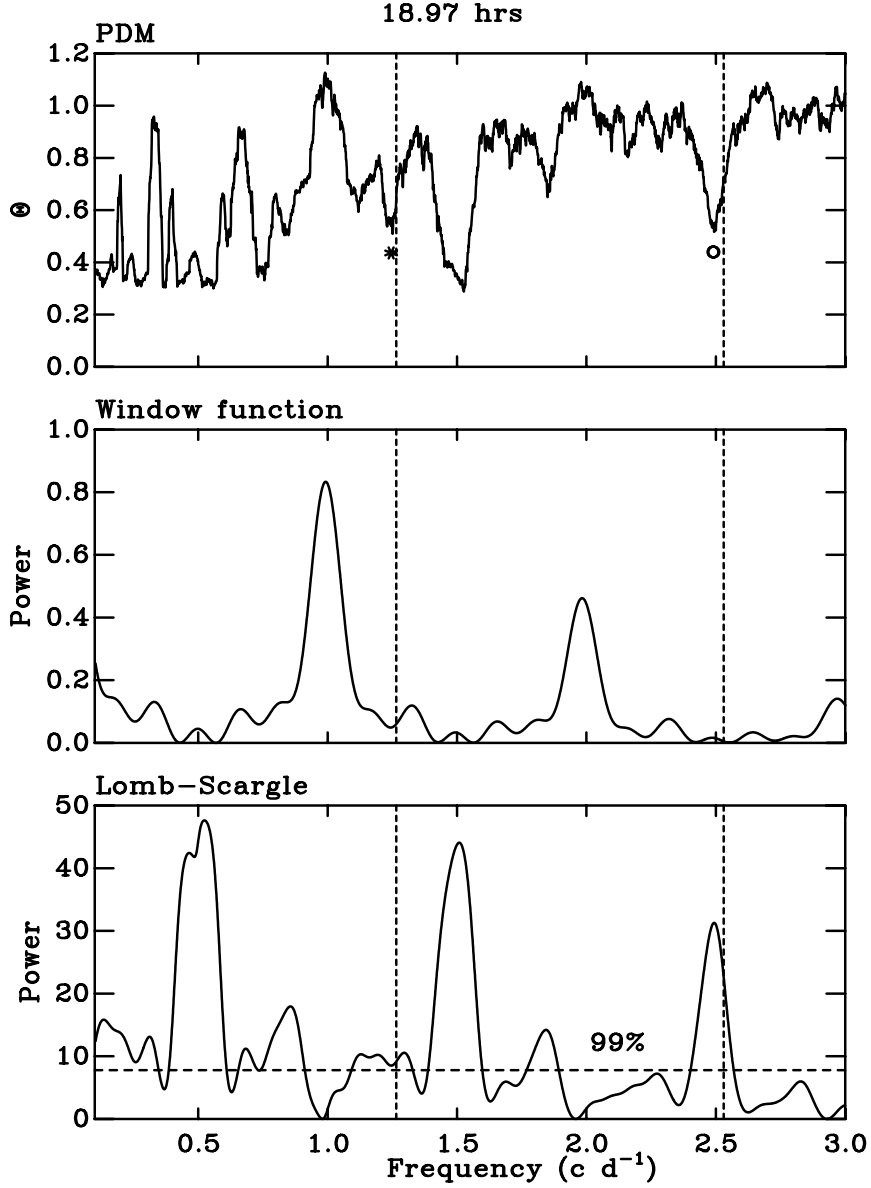


Figure 1. Results of the period search using the *I*-band data of Aql X-1 during quiescence. *Top*: Phase Dispersion Minimization (PDM) periodogram. The frequency 1.242 c d^{-1} which we interpret as the orbital frequency is marked with a star; twice this frequency is also shown (white circles). *Middle*: Window function. *Bottom*: Lomb-Scargle power spectrum. The vertical dashed line is the orbital period determined by Chevalier & Ilovaisky (1991) at 18.97 hr. A Monte Carlo simulation provides the 99 per cent confidence level, shown as the dashed horizontal line. We interpret the periodicity at 2.487 c d^{-1} , present in the Lomb-Scargle and PDM periodograms, as twice the orbital frequency (see text), since it is consistent with twice Chevalier & Ilovaisky's orbital frequency.

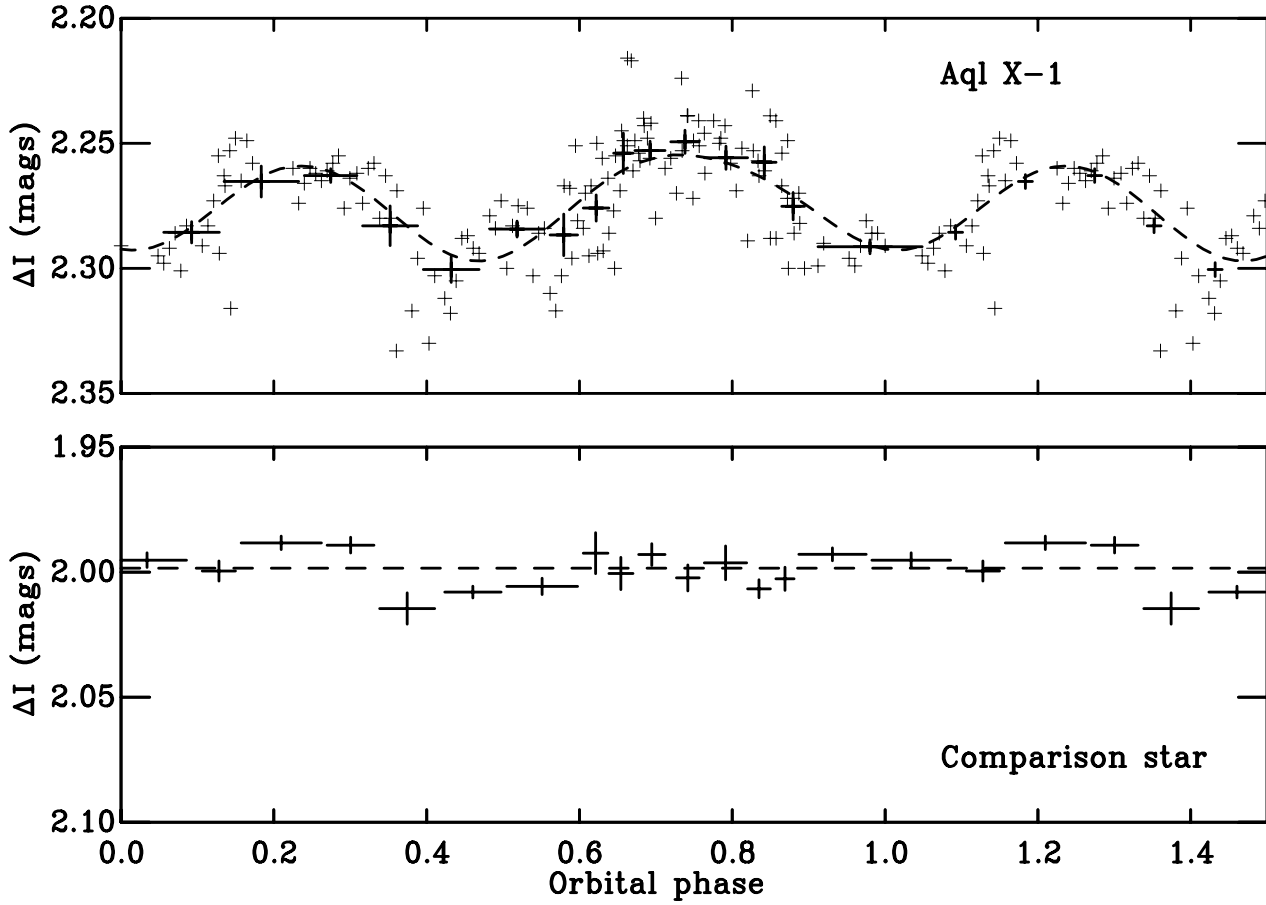


Figure 2. The phase-binned light curves for Aql X-1 (top) and a comparison star (bottom). In the top panel we also show the phase-folded data for Aql X-1 (light weighted crosses). The dotted line in the comparison star light curve is a linear fit. The best fit ellipsoidal model (dashed line) at $q = 3$ and $i = 25^\circ$ is shown in the light curve of Aql X-1. We show 1.5 orbital cycles for clarity.

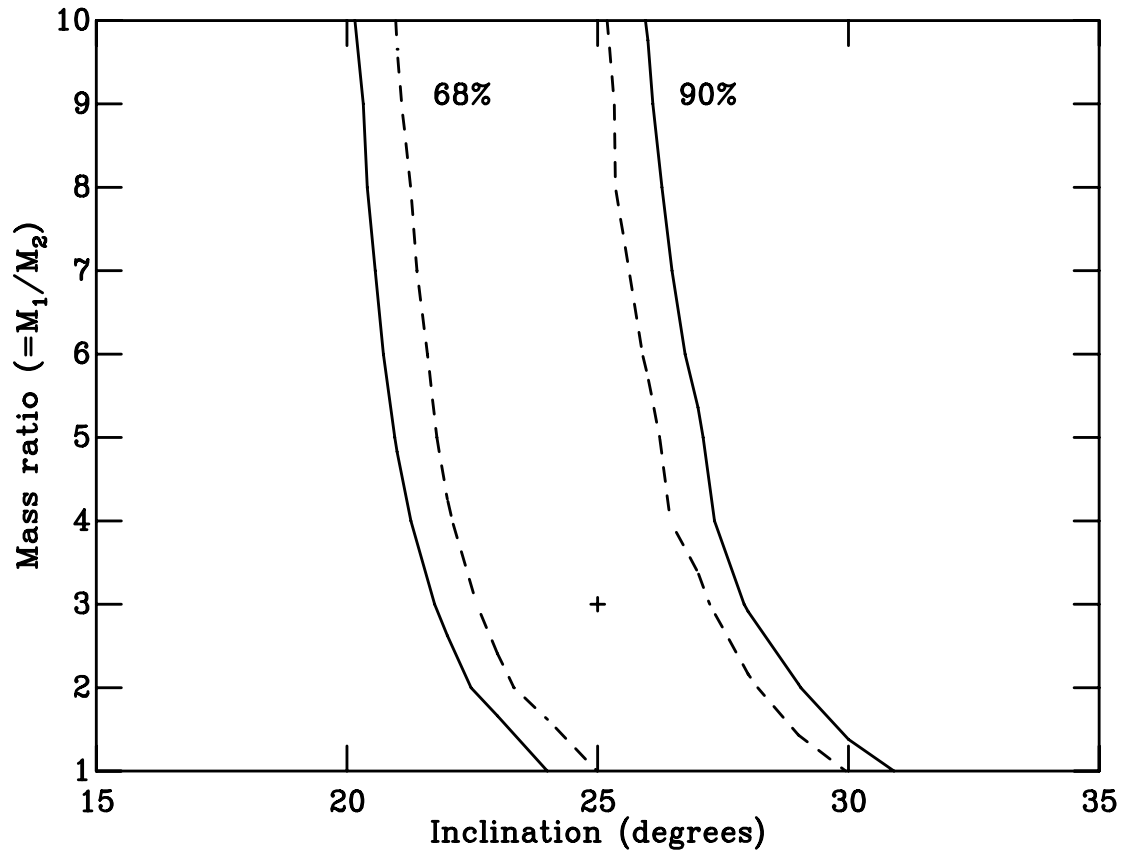


Figure 3. The 68 and 90 per cent confidence level solutions for the ellipsoidal model fits to the Aql X-1 *I*-band light curve. The cross marks the best solution.